DOI: 10.1002/ ((please add manuscript number))
Article type: Full Paper

Highly tunable polarized chromatic plasmonic films based on sub-wavelength grating templates

Jun Zheng, Zhi-Cheng Ye, Cheng-Liang Wang, Yi-Fei Fu, Xin-Ran Huang and Zheng-Ming Sheng*

Jun Zheng and Xin-Ran Huang
Key Laboratory for Laser Plasmas (Ministry of Education), School of Physics and astronomy, and Collaborative Innovation Center of IFSA (CICIFSA), Shanghai Jiao Tong University, Shanghai, 200240, China
E-mail: jzheng@sjtu.edu.cn
Zhi-Cheng Ye, Cheng-Liang Wang, and Yi-Fei Fu
Department of Electronic Engineering, Shanghai Jiao Tong University, Shanghai, 200240, China
Zheng-Ming Sheng
SUPA and Department of Physics, University of Strathclyde, Glasgow G4 0NG, UK
Key Laboratory for Laser Plasmas (Ministry of Education), School of Physics and astronomy, and Collaborative Innovation Center of IFSA (CICIFSA), Shanghai Jiao Tong University, Shanghai, 200240, China

Keywords: plasmonic structural colors, sub-wavelength grating, metallic nanowire gratings, polarizer, color filter

A kind of polarized chromatic plasmonic film is proposed based on sub-wavelength grating structure, which enables ‘blue transmission’ for the transverse electric (TE) light and ‘red transmission’ for the transverse magnetic (TM) light. Metal-insulator-metal plasmonic waveguiding and metallic nanowire scattering are revealed to be responsible for the chromatic shift. Based upon the unique transmission spectrum characteristics of such films, polarized chromatic plasmonic tags (PCPTs) can be flexibly fabricated by patterning dielectric grating templates with designed figures and depositing appropriate thickness of metal. These PCPTs, simultaneously possessing directly visible unpolarized transmission colors and concealed distinct polarization-dependent color shift, can be widely used as anti-counterfeiting tags with higher security than the diffractive types of holograms.

1. Introduction

Metallic nanoarray based plasmonic structutral color (PSC) has been widely investigated as colorfilters,[1-3] polarizers,[4-6] and highly sensitive surface plasmon resonance sensors.[7] The devices based on PSC have the advantages of longer lifetime, thinner dimension, better performance than the conventional types, which can be widely used in displays, anti-counterfeiting,[8, 9] and image sensors.[10] Generally, the functions of metallic nanoarrays are realized by the following three mechanisms: (1) the localized surface plasmon resonance in metallic nano-units, which leads to absorption dips in the transmission or reflection;[11, 12] (2) the surface plasmon spoofed by the nanoarrays, which lead to extraordinary transmission through dielectric apertures below diffraction limits;[13, 14] (3) the plasmonic waveguiding of dielectric slits, which supports broadband polarized transmission of TM light, while prohibits the propagation of TE light.[15] Utilizing these mechanisms, the spectra of metallic nanoarray can be flexibly tuned to meet a variety of applications by engineering the metal thickness, profile of the unit cells, and the period. For example, by tailoring the profile of the nano unit cell to be asymmetric (linear, elliptical, or rectangular), polarization-dependent tunability can be imposed on the PSC to make integrated colorfilters and polarizers[16, 17] for more compact and lower-power-consumption liquid crystal displays (LCDs). Recently, actively tunable PSCs based on elastomeric substrates have been reported. By stretching the substrates, the pitch and therefore scattering colors of PSCs can be modified in a wide range, showing great promising as novel display devices.[18] Besides the structure, the permittivity of the metal materials also strongly affects the spectrum characteristics. For instance, with small damping factors, gold and silver metallic nanoarrays have sharp surface plasmon resonance dips that suitable for high figure of merit bio-sensing.[19] While aluminium (Al) has a large absolute value of complex permittivity and a large plasmon frequency to maintain plasmonic characteristics at wavelength down to ultraviolet, thus it is suitable to make broadband

nanowire polarizers with high extinction ratio of TM over TE light in the transmission. In addition, Al has been widely used in the packaging, decoration, and laser hologram tags to enhance the reflection of diffraction gratings.[19-21]

In this work, we propose a kind of transmission films of one-dimensional metallic nanowire gratings (MNGs), which show polarization-dependent PSC over broad spectrum. Such films can be used as a new type of high-security and more recognizable anti-counterfeiting tags: polarized chromatic plasmonic tags (PCPTs). The physical mechanisms responsible for the polarization-dependent chromaticity are revealed, which are used in the device design. In Section. 2, the fabrication of the films and tags is presented and their transmission spectra are described as a function of the MNG parameters and incident light parameters. In Section 3, a physical model is presented to decribe the polarization-dependent chromaticity. The paper concludes with a summary in Section 4.

2. Device fabrication and spectra measurements

2.1. Device fabrication and basic principle

As shown in **Figure 1**, the fabrication procedure of MNG-based PCPT includes three steps. Firstly, dielectric grating templates are fabricated by using laser interference lithography (LIL)[22] or nano-imprinting lithography (NIL), which have shown the advantages in the mass production of MNGs. Then, the figures of tags are patterned on the templates by using flexible mask-free laser engraving or rapid mask-based UV printing. Finally, by depositing appropriate thickness of Al, the demanded colors of the plasmonic tags are obtained, where only gratings in the figures of interest are remained. The diffractive snapshots of the samples fabricated in each step are presented in Figure 1(a3), (b3), and (c3).

A schematic diagram of the MNG forming the PCPTs is illustrated in **Figure 2**(a). The device includes three layers of gratings: top Al-air, middle photoresist (PR) bar (coated with a thin layer of Al on the sidewalls)-air, and bottom PR-Al gratings. A collimated white light beam is incident to the device with angle of θ. The incident plane is perpendicular to the grating lines. The TE light with shorter wavelength and TM light with longer wavelength are transmitted through the film as shown by the colored arrows. The scanning electronic microscopy (SEM) images of the fabricated PCPT are shown in Figure 2(b), where the grating was fabricated by using NIL on a glass substrate with pitch T = 180 nm, width of the PR t_1 = 120 nm, and thickness of PR h_2 = 130 nm. After the patterning of the logo of Shanghai Jiao Tong Universtiy by using laser engraving, Al of 10 nm in thickness was conformally deposited on the dielectric grating.

As displayed in Figure 2(c), the measured transmittance of TE and TM lights have a peak in the 'blue' region with wavelength of 420 nm (blue line) and 'red' region with wavelength of 770 nm (red line), respectively. More specifically, the measured TM transmittance T_{TM} is 1.2% at wavelength 420 nm and 29% at wavelength 770 nm, while the transmittance of TE light T_{TE} at these two wavelengths are 32% and 3.8%, respectively. It means the extinction ratio T_{TE}/T_{TM} is about 27 at wavelength 420 nm, and the extinction ratio T_{TM}/T_{TE} is about 8 at wavelength 770 nm. Due to the high contrast ratios between the peaks and valleys of the two orthogonal polarizations, noticable polarization-dependent color shifts can be obtained.

The measured polarization-dependent transmitted spectra are shown in Figure 2(c), which can be represented by $T(\lambda, \varphi) = T_{TM}(\lambda)\cos^2\varphi + T_{TE}(\lambda)\sin^2\varphi$, where λ is the wavelength of light in free space and φ is the cross angle between the electric vector with the incident plane. It is φ = 0^o for TM polarization and 90^o for TE polarization. The corresponding chromaticity mapped as red points in the CIE 1931 xy chromaticity diagram in Figure 2(d) further illustrates the

distinct color shifts. The snapshots of the PCPT are shown in Figure 2(e), where the color shifts from golden to blue are vividly displayed as the polarization of the incident white light is rotated from TM (φ=0^o) to TE (φ=90^o). The video of the transmission can be found in the supplementary information of this paper. One may note that the color for the case of φ=45^o is the same with that produced by unpolarized light, which means that decorative colorful pictures (purple in this case) can be directly observed without polarizers.

2.2. Characterization of the transmission spectra

As shown in Figure 2(c), there is a intersection point wavelength λ_c, where $T_{TM}(\lambda_c) = T_{TE}(\lambda_c)$. This can be used to evaluate the color difference between TE and TM lights, i.e., TE transmittance is higher than that of TM for $\lambda<\lambda_c$, and TM transmittance is higher than TE for $\lambda>\lambda_c$. Thus the 'blue' component in the transmitted color is mainly determined by TE light, and the 'red' part is mainly decided by TM light. In **Figure 3**(a), λ_c is showed as a function of Al thickness h_1 and grating pitch T, calculated by using RSOFT and DiffractMOD^{TM}. Generally, with the increase of h_1 or decrease of T, λ_c moves to shorter wavelengths, leading to the blue shift of the peaks for TE light and the broadening of the spectra for TM light. Besides the shift of λ_c, as shown in Figure 3(b), the TE transmission is weakened and the TM transmission at the shorter wavelengths is enhanced when the thickness of the Al layer is increased. This is due to the increasing inhibition and enhancement effects to TE and TM light, respectively, via plasmonic waveguiding.[23] For Al thickness h_1 of 80 nm, the transmission of TM light displays a white color with spectra entirely covering the visible lights, while the TE light exihibits black due to the weak transmittance of less than 0.01%. The giant change of the transmitted colors from chromtic to black and white with the increasing Al thickness well illustrates the high tunability of the MNG-based PSC.

The schematic diagram and experimental results for the grating with Al thickness of 60 nm are shown in **Figure 4**. The transmitted spectra conspicuously show broadband polarization features with extinction ratio of T_{TM}/T_{TE} reaching 40~140 in the whole visible lights. The images of the characters 'SJTU' composed of thick-Al MNG in Figure 4(b) further display bright and dark transmission for TM and TE light, respectively.

A variety of 'blue' TE and 'red' TM transmission of PCPTs with different Al thickness and grating pitch are shown in **Figure 5**, which can display the high tunability of the chromatic characteristics of MNG-based PSC. At first, photoresist gratings with pitches of 350, 300 and 260 nm are fabricated on BK7 glass substrates as templates by using LIL. Then the templates are patterned with figures by using UV-printing, where only gratings are remained in the logos. Finally, a layer of Al film is deposited on the logos to make PCPTs. In LIL, the corresponding cross angles between the two laser beams (He–Cd laser, wavelength 442 nm, KIMMON) are of 78^o, 95^o, and 116^o, respectively.

As shown by the measured spectra for T= 350 nm with h_1 = 15 and 40 nm in Figures 5(a1) and 5(a2), respectively, λ_c is blue-shifted with increasing thickness of Al film. Moreover, their shifts of chromaticity with the incident light polarizations behave distinctly different, as mapped in Figure 2(d). The transmitted color and λ_c can also be adjusted by the grating pitch as shown in Figures 5(a2-a4) for T= 350, 300 and 260 nm. The shorter the pitch, the shorter the wavelength λ_c, in agreement with the simulation results in Figure 3(a). The corresponding simulated spectra and colors for TM and TE cases are presented with dashed lines in Figure 5(a) and circle markers in Figure 2(d) for comparison. The simulated transmittance is about twice of the experimental results. A series of experimental snapshots in Figure 5(b) vividly show the variations of the logo colors under different Al thickness and grating pitch. The pictures in the dashed rectangle are the same with those observed under unpolarized white

light. Related with this figure, four videos showing the light transmission are given in the supplementary information. In general, by changing the thickness of the metal layer and the grating pitch, preferable colors, as well as the color shift tendency with light polarization, are achievable.

3. Analysis of the physical mechanisms

Single nanowire resonant scattering,[24] mutual nano-gap coupling[25] and waveguiding of metal-insulator-metal nano-slits[26, 27] have been commonly known to be the main mechanisms determining the spectral characteristics of MNGs. However, the phenomena of 'blue' TE and 'red' TM- polartized chromatic tranmission found in this work have not been investigated. To understand how the plasmonic effects lead to such a large optical anisotropy, we plot the dispersion curves of the slit modes of the three layers of the MNGs in **Figure 6** based upon our previous model[26]. Here the blue stars and red dots represent the real (k_{zr}) and imaginary (k_{zi}) parts of the wave number k_z, respectively. From these curves we can deduce: (1) Due to the negligible imaginary parts k_{zi} of the wavenumber, TM light can pass through the top and bottom Al grating layer in plasmonic waveguide modes beyond diffraction limit. (2) The TE light in the top and bottom Al grating layers is lossy because $k_{zi} >> k_{zr}$. The larger the wavelength, the higher lossy the TE light, because of the increasing k_{zi} with wavelength.

Besides the plasmonic waveguiding effect, the inherent scattering of metallic nanowires cannot be ignored. The forward scattering cross-sections (S_f) of the MNGs with pitch of 180 nm are shown in **Figure 7**, which is calculated by LUMERICAL, FDTD Solutions^{TM}. For h_1= 10 nm in Figure 7(a), S_f shows obvious wavelength dependence for both polarizations. S_f of TE light at wavelengths shorter than λ_c is larger than that of TM light. S_f of TM light at wavelengths longer than λ_c is larger than that of TE light. For h_1= 60 nm in Figure 7(b), the

wavelength dependence of S_f for TM light fades. But the value of S_f is generally increased. The wavelength dependence of S_f for TE light is kept, while it is less than that of TM light in the whole range of visible lights, especially at the longer wavelengths.

Combining both plasmonic waveguiding and scattering effects, we can conclude: (1) In the thin metal case, TE light with shorter wavelength can still penetrate into the top and bottom layer of metallic gratings in the form of evanescent wave, while TM light with the same wavelengths suffers from metallic nanowire scattering as shown in Figure 7(a). Thus TE light has higher transmittance than TM light at the shorter wavelength; (2) With the increase of Al thickness, the plasmonic waveguiding effect gradually dominates, thus TE light only with much shorter wavelength can penetrate into the metallic gratings, while the TM light can transmit efficiently.

The transmittance can also be tuned by varying the thickness of the middle dielectric layer based on the well-known Fabri-Perrot (F-P) resonance effect, as shown by the transmission for wavelength 400 nm in **Figure 8**. The main inherent difference between the TM and TE polarizations caused by the waveguide effect is asssociated with the effective refractive index. The real part of effective refractive indexes n_{eff} in the three layers have the relations $n_{eff\_top} < n_{eff\_mid} < n_{eff\_bot}$ for TM light and $n_{eff\_mid} > n_{eff\_top}$, n_{eff_bot} for TE light, according to the dispersion relations shown in Figure 6. It means that there is a phase difference of π between TM and TE caused by the interface reflectance. Thus the resonant wavelengths of the peaks for both polarizations are different. Although F-P effect can effectively tune the transmitance, there is always T_{TE} (dashed blue line) > T_{TM} (dashed voilet line) for small h_2 and T_{TE} (solid blue line) < T_{TM} (solid voilet line) for large h_2. Obviously, the 'blue' TE and 'Red' TM polarized chromatic transmission is mainly decided by the metallic thickness h_1 other than by the dielectric thickness h_2. The different effects of metal thickness and dielectric grating height to the spectra properties of MNGs help to break through the restriction in designing

PCPTs where the transmittance and colors are shifted simultaneously by only tuning the metal thickness.

4. Summary

We have proposed a type of MNG films, which enables to show directly colors under the irradiation of unpolarized ambient white light. Moreover, it can display polarization-dependent color shifts. Plasmonic waveguiding of the slits and scattering of the metallic nanowries are revealed to be responsible for the characteristics of 'blue' TE and 'red' TM polarized transmission. The MNG-based PCPT has the following characteristics: (1) The grating pitch is sub-wavelength-scale, which can efficiently prevent unauthorized duplicating by using laser writing technology that micrometer-scaled hologram tags suffer from; (2) The transmitted colors can be flexibly tuned by engineering the metal thickness or grating pitch. (3) The transmitted colors deduced by plasmonic effect is distinctly different from the angle-dependent diffraction of holograms; (4) Even further, the concealed polarized chromaticity can significantly raise the security level of anti-counterfeiting tags.

The massive fabrication of such MNG film based PCPTs has been achieved. The procedure includes: sub-wavelength grating templates fabrication by NIL and LIL, figure patterning by laser engraving or UV-printing, and PSC engineering by depositing appropriate thickness of Al. The MNG-PCPTs can also be produced flexibly with demanded colors. Possessing the advantages of dramatic polarized color shift, much finer structure and compatible technology with present industrial capabilities, MNG-PCPTs are deemed to be readily applicable in the market of commercial tags, which have much higher securiety than the current diffractive hologram tags.

Supporting Information
Supporting Information is available from the Wiley Online Library or from the author.

Acknowledgements
This work was supported by the National Natural Science Foundation of China (Nos. 61775136 and 11721091)

Received: ((will be filled in by the editorial staff))
Revised: ((will be filled in by the editorial staff))
Published online: ((will be filled in by the editorial staff))

References

[1] Q. Chen and D. R. S. Cumming, *Opt. Express* **2010**, *18*, 14056.

[2] H. S. Lee, Y. T. Yoon, S. S. Lee, S. H. Kim and K. D. Lee, *Opt. Express* **2007**, *15*, 15457.

[3] Y. Liang, W. Peng, M. Lu and S. Chu, *Opt. Express* **2015**, *23*, 14434.

[4] Z. Yu, P. Deshpande, W. Wu, J. Wang and S. Y. Chou, *Appl. Phys. Lett.* **2000**, *77*, 927.

[5] X. P. Zhang, H. Liu, J. Tian, Y. Song and L. Wang, *Nano Lett.* **2008**, *8*, 2653.

[6] T. Weber, T. Käsebier, A. Szeghalmi, M. Knez, E. Kley and A. Tünnermann, *Nanoscale Res. Lett.* **2011**, *6*, 558.

[7] J. N. Anker, W. P. Hall, O. Lyandres, N. C. Shah, J. Zhao and R. P. V. Duyne, *Nat. Mater.* **2008**, *7*, 442.

[8] J. Sauvage-Vincent, S. Tonchev, C. Veillas, S. Reynaud and Y. Jourlin, *Europ. Opt. Soc. Rap. Public.* **2013**, *8*, 13015.

[9] E. L. Prime and D. H. Solomon, *Angew. Chem. Int. Ed.* **2010**, *49*, 3726.

[10] S. Yokogawa, S. P. Burgos and H. A. Atwater, *Nano Lett.* **2012**, *12*, 4349.

[11] E. Hutter and J. H. Fendler, *Adv. Mater.* **2012**, *16*, 1685.

[12] K. A. Willets, A. J. Wilson, V. Sundaresan and P. B. Joshi, *Chem. Rev.* **2017**, *117*, 7538.

[13] K. A. Willets, A. J. Wilson, V. Sundaresan and P. B. C. Genet and T. Ebbesen, *Nature* **2007**, *445*, 39.

[14] N. L. Sun, J. Cui, Y. She, L. Lu, J. Zheng and Z. C. Ye, *Opt. Mater. Express* **2015**, *5*, 912.

[15] J. Zheng, Z. C. Ye, N. L. Sun, R. Zhang, Z. M. Sheng, H. P. Shieh, and J. Zhang, *Sci. Rep.* **2014**, *4*, 6491.

[16] E. Laux, C. Genet, T. Skauli and T. W. Ebbesen, *Nat. Photonics* **2008**, *2*, 161.

[17] T. Xu, Y. Wu, X. Luo and L. Guo, *Nat. Commun* **2010**, *1*, 1058.

[18] M. Tseng, J. Yang, M. Semmlinger, C. Zhang, P. Nordlander and N. Halas, *Nano Lett.* **2017**, *17*, 6034.

[19] N. L. Dmitruk, M. Klopeleisch, O. I. Mayeva, S. V. Mamykin, E. F. Venger and O. B. Yastrubchak, *Phys. Stat. Sol.(a)* **2001**, *184*, 165.

[20] F. M. Tuffy, *Proceedings of SPIE* **2000**, *3973*, 231.

[21] T. Velten, F. Bauerfeld, H. Schuck, S. Scherbaum, C. Landesberger and K. Bock, *Microsyst. Technol.* **2011**, *17*, 619.

[22] S. Song, X. Ma, M. Pu, X. Li, K. Liu, P. Gao, Z. Zhao, Y. Wang, C. Wang and X. Luo, *Adv. Opt. Mater.* **2017**, *5*, 1600829.

[23] Szeghalmi, M. Helgert, R. Brunner, F. Heyroth, U. GÖsele and M. Knez, *Adv. Funct. Mater.* **2010**, *20*, 2053.

[24] T. Sondergaard and S. I. Bozhevolnyi, *Opt. Express* **2007**, *15*, 4198.

[25] D. C. Skigin and R. A. Depine, *Phys. Rev. Lett.* **2005**, *95*, 217402.

[26] Z. C. Ye, J. Zheng, S. Sun, L. D. Guo and H. P. D. Shieh, *IEEE J. Sel. Top. Quant. Elec.* **2013**, *19*, 4800205.

[27] D. Wan, H. Chen, Y. Lai, H. Yu and K. Lin, *Adv. Funct. Mater.* **2010**, *20*, 1742.

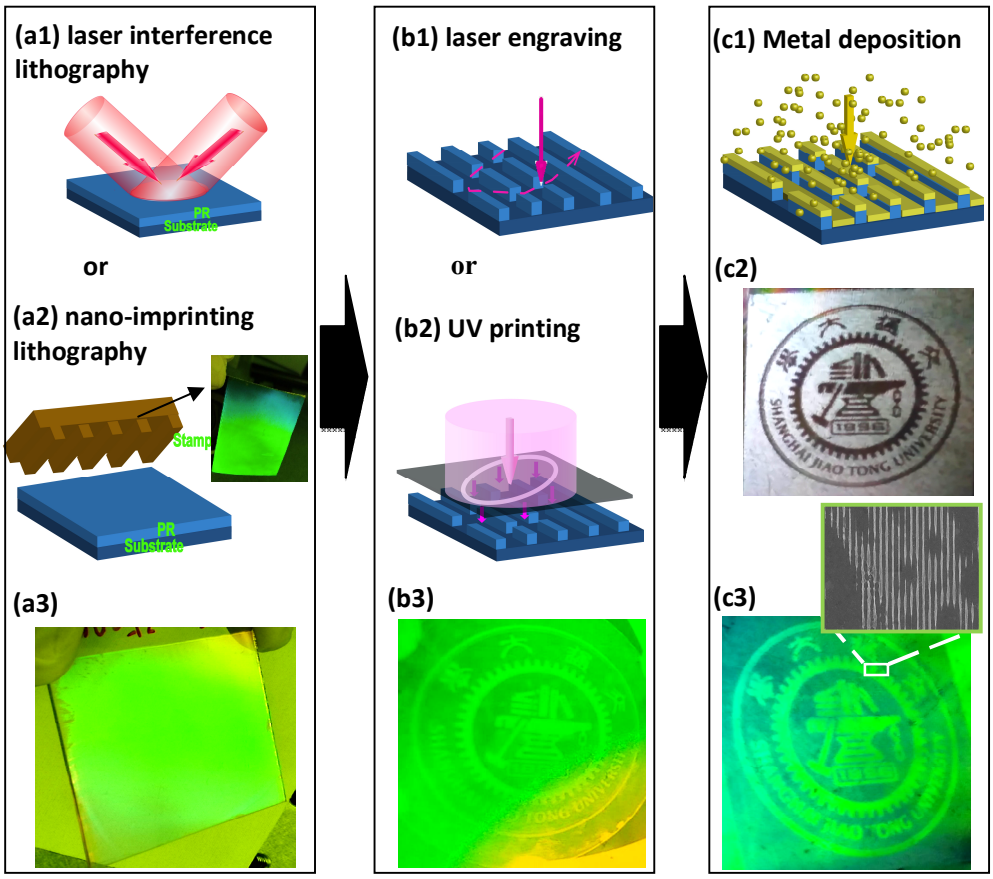

Figure 1. The Fabrication procedure of the proposed MNG-based PCPT. Firstly, dielectric grating templates are fabricated by using LIL (a1) or NIL (a2). A diffractive snapshot of a nickel stamp is presented in (a2). Then, the figures of tags are patterned on the templates by using direct mask-free laser engraving (b1) or rapid mask-based UV printing (b2), where only gratings in the figures are kept. Finally, by depositing appropriate thickness of Al (c1), the demanded colors of the plasmonic tags are obtained. A reflective snapshot of the final PCPT is presented in (c2). Diffractive snapshots of the fabricated samples in each step are presented in (a3, b3, c3). A SEM image is presented in (c3) as well, which clearly displays that only gratings are remained in the figures.

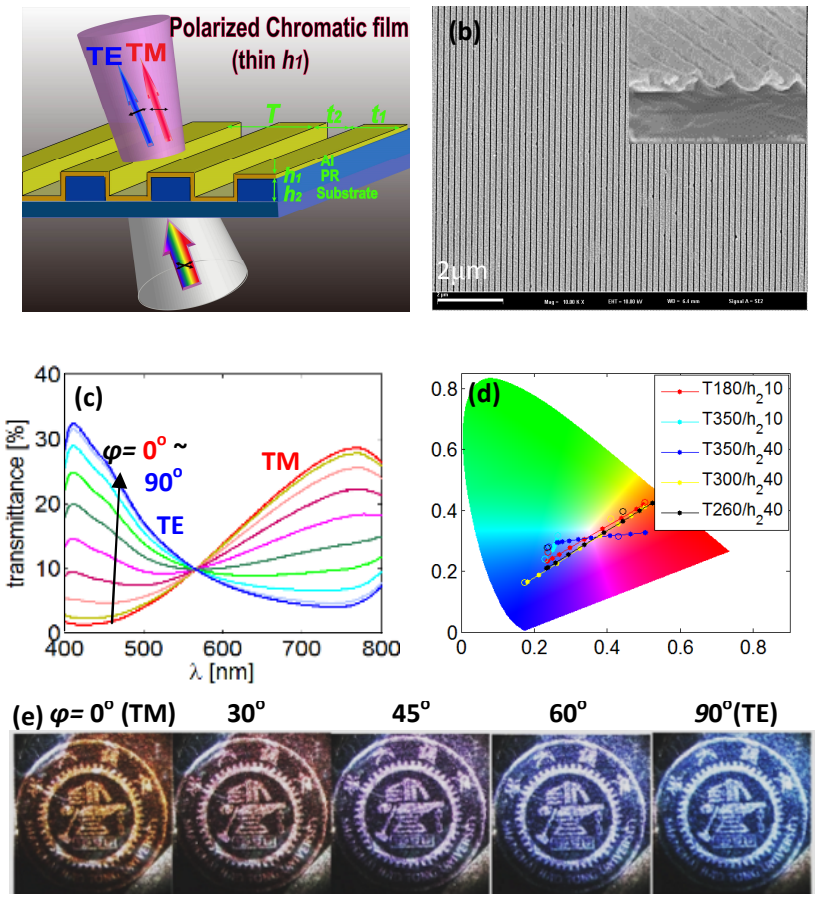

Figure 2. The structure and measured transmission of the fabricated MNG-based PCPTs. (a) The schematic diagram of the MNG. (b) The top and side (inset) SEM images of the fabricated MNGs with pitch of 180 nm. (c) Polarization-dependent transmitted spectra with light incident angle θ= 0° and the polarization angle φ from 0° (TM, red line) to 90° (TE, blue line) at a step of 10°. (d) The spectra's corresponding points in the CIE 1931 xy chromaticity diagram. The measured (the color lines with solid dots) and simulated (the circles) color shifts of the devices with the variation of light polarizations under different grating pitch T and Al thickness h_1. The red and other color points correspond to the spectra in (c) and Figure 5(a), respectively. (e) Snapshots of the fabricated PCPT illuminated by white light with different polarization state. represent

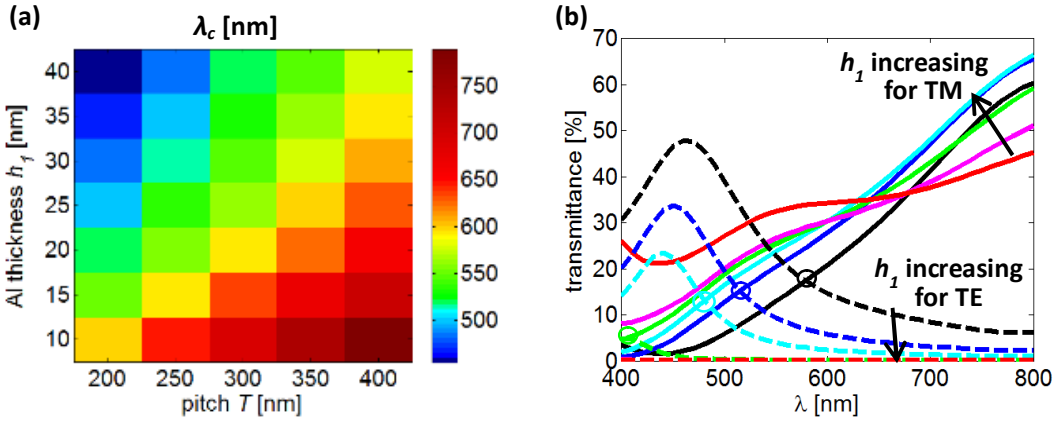

Figure 3. Dependence of λ_c on Al thickness h_1 and grating pitch T. (a) Simulation results of λ_c varying with h_1 and T, where dielectric thickness h_2= 130 nm and width t_1= T/2. (b) Calculated TM (solid lines) and TE (dashed lines) transmittance for the grating with h_1=10, 15, 20, 40, 60, and 80 nm. The circle markers indicate λ_c. Other parameters are the same with that in Figure 2.

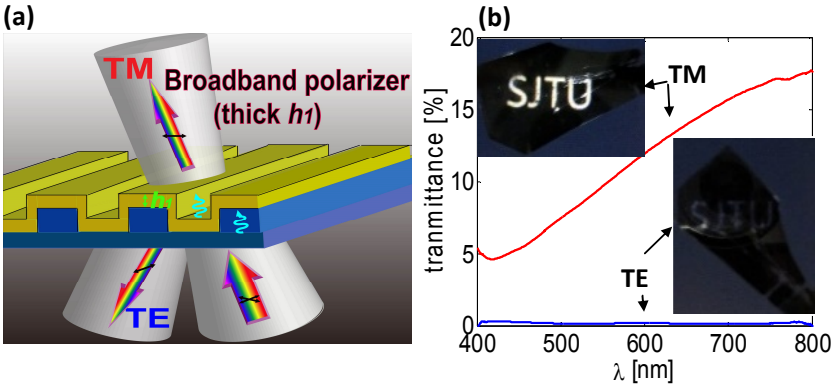

Figure 4. PCPT with a thick Al layer. (a) The schematic diagram of the MNG acting as a broadband polarizer. The blue wave curves in the PCPT represent the longitudinal plasmonic slit-waveguide mode, which is the primary physical component responsible for the polarization dependent transmission. (b) The measured TM (red line) and TE (blue line) transmissions for a grating with Al thickness h_1= 60 nm, and the other parameters are the same with those in Figure 2(b). The snapshots illustrate the transmitted bright TM and dark TE polarized colors of the characters of "SJTU" composed of MNGs.

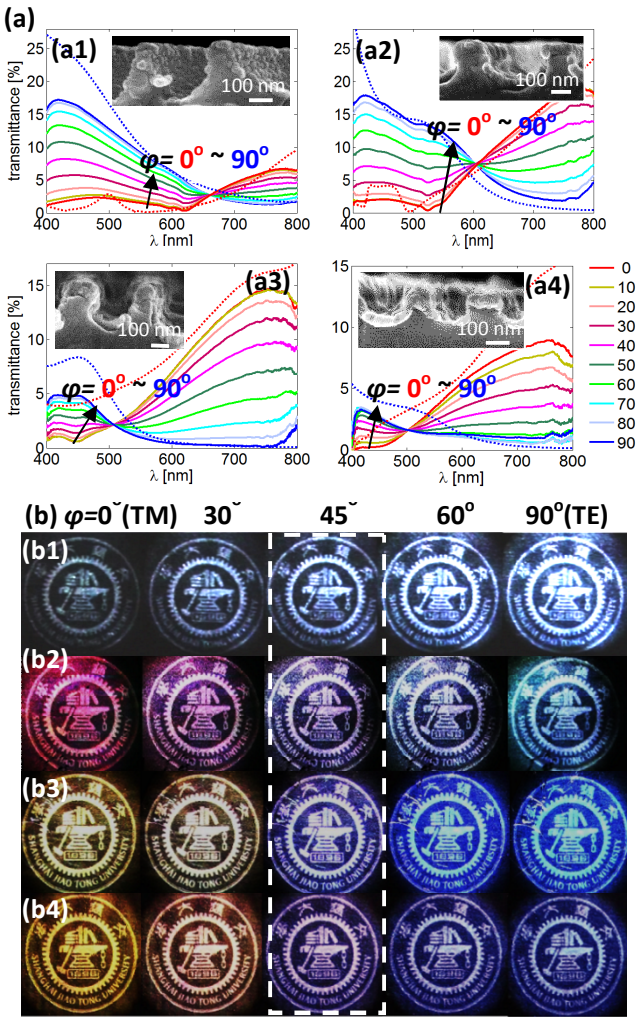

Figure 5. Polarization-dependent transmission measured experimentally with different Al thickness h_1 and grating pitch T. (a) Transmission spectra with polarization angle φ varying from 0^o to 90^o at a step of 10^o. The solid lines are experimental results. The blue and red dashed lines are the simulated results for $\varphi=0^o$ and 90^o, respectively, whose intensity are divided by 2 for clear comparison with the experimental results. The insets are the side SEM images of the PCPTs. (b) The snapshots of PCPTs for different polarization states, where the pictures within the dashed rectangle are the same with those observed under unpolarized light. Following are the corresponding parameters for the PCPTs: (a1, b1) T= 350 nm, h_1 = 15 nm; (a2, b2) T= 350 nm, h_1= 40 nm; (a3, b3) T= 300 nm, h_1= 40 nm. (a4, b4) T= 260 nm, h_1= 40 nm. The dielectric thickness h_2= 150 nm and width t_1= 0.5T.

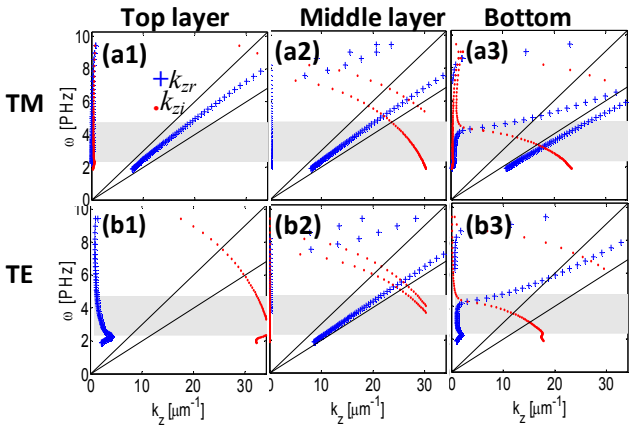

Figure 6. Dispersion curves of the waveguides in three layers of the MNGs: (a1, b1) the air-Al-air grating in the top layer, (a2, b2) the air-PR-air grating in the middle layer and (a3, b3) the Al-PR-Al grating in the bottom layer, where (a1-a3) are for TM light and (b1-b3) are for TE light. The black lines represent the PR and air lines. The gray regions highlight the visible light zone. Simulation parameters are the same as that in Figure 2.

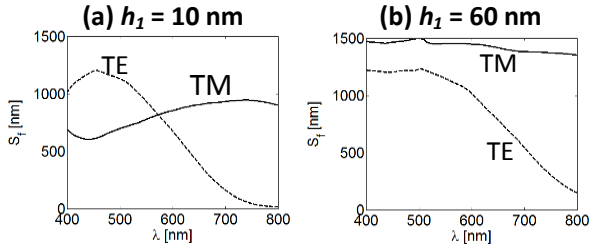

Figure 7. The forward scattering cross-section (S_f) for pitch T=180 nm and Al thickness (a) h_1=10 nm and (b) h_1=60 nm. Other simulation parameters are the same as that in Figure 2.

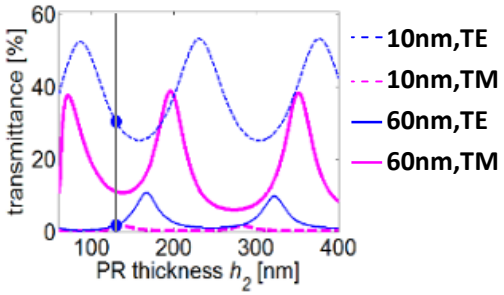

Figure 8. Transmittance varying with PR thickness obtained from simulaiton. The transmittance for TM (solid lines) and TE (dashed lines) light with wavelength of 400 nm in case of pitch T=180 nm and Al thickness h_1= 10 nm (blue lines) and 60 nm (violet lines). The black vertical line represents the case in our fabricated device with the PR thickness h_1=130 nm. Other simulation parameters are same with that in Figure 2.

The table of contents entry should be 50–60 words long, and the first phrase should be bold. The entry should be written in the present tense and impersonal style. The text should be different from the abstract text.

Keywords: plasmonic structural colors, sub-wavelength grating, metallic nanowire gratings, polarizer, color filter

Jun Zheng*, Zhi-Cheng Ye, Cheng-Liang Wang, Yi-Fei Fu, Xin-Ran Huang and Zheng-Ming Sheng

Highly tunable polarized chromatic plasmonic films based on sub-wavelength grating templates

ToC figure ((Please choose one size: 55 mm broad × 50 mm high **or** 110 mm broad × 20 mm high. Please do not use any other dimensions))

A polarized chromatic plasmonic film is proposed based on sub-wavelength grating structure, which enables 'blue transmission' for the transverse electric (TE) light and 'red transmission' for the transverse magnetic (TM) light. Based upon the unique transmission spectrum characteristics of such films, polarized chromatic plasmonic tags (PCPTs) with demanded versatile polarized transmission colors can be fabricated in a large scale.